Representation of Soil Moisture Feedbacks during Drought in NASA Unified WRF (NU-WRF)

BENJAMIN F. ZAITCHIK

Department of Earth and Planetary Sciences, The Johns Hopkins University, Baltimore, Maryland

JOSEPH A. SANTANELLO

Hydrological Sciences Laboratory, NASA Goddard Space Flight Center, Greenbelt, Maryland

SUJAY V. KUMAR

Hydrological Sciences Laboratory, NASA Goddard Space Flight Center, and Science Applications International Corporation, Greenbelt, Maryland

CHRISTA D. PETERS-LIDARD

Hydrological Sciences Laboratory, NASA Goddard Space Flight Center, Greenbelt, Maryland

(Manuscript received 16 May 2012, in final form 16 August 2012)

ABSTRACT

Positive soil moisture–precipitation feedbacks can intensify heat and prolong drought under conditions of precipitation deficit. Adequate representation of these processes in regional climate models is, therefore, important for extended weather forecasts, seasonal drought analysis, and downscaled climate change projections. This paper presents the first application of the NASA Unified Weather Research and Forecasting Model (NU-WRF) to simulation of seasonal drought. Simulations of the 2006 southern Great Plains drought performed with and without soil moisture memory indicate that local soil moisture feedbacks had the potential to concentrate precipitation in wet areas relative to dry areas in summer drought months. Introduction of a simple dynamic surface albedo scheme that models albedo as a function of soil moisture intensified the simulated feedback pattern at local scale—dry, brighter areas received even less precipitation while wet, whereas darker areas received more—but did not significantly change the total amount of precipitation simulated across the drought-affected region. This soil-moisture-mediated albedo land–atmosphere coupling pathway is structurally excluded from standard versions of WRF.

1. Introduction

Mechanisms of soil moisture–precipitation feedbacks affecting climate have been the subject of conceptual (Betts and Ball 1998; Eltahir 1998; Findell and Eltahir 2003; Seneviratne et al. 2006; Teuling et al. 2010), modeling (Charney et al. 1977; Dirmeyer et al. 2006; Koster et al. 2004; Meng et al. 2011; Pielke et al. 1999; Santanello et al. 2011; Weaver et al. 2002; Zaitchik et al. 2007), and observational (Notaro et al. 2006; Seneviratne and Stockli 2008; Taylor and Lebel 1998) analyses. These investigations show that soil moisture conditions and vegetation status can influence temperature, humidity, winds, and precipitation at local to global scale and subdaily to seasonal time scales. This is particularly true in transitional climate zones, including the U.S. southern Great Plains (SGP), where significant soil moisture variability, moisture-sensitive evaporation rates, and potential for convective instability lead to strong land–atmosphere coupling (Koster et al. 2004; Seneviratne et al. 2006; Teuling et al. 2009). Seneviratne et al. (2010) and Betts (2009) provide reviews of this rapidly evolving field.

The SGP has been the test site for several seminal studies of soil moisture feedbacks. These include the complementary First International Satellite Land Surface

Corresponding author address: Benjamin F. Zaitchik, 3400 N. Charles St., 301 Olin Hall, Baltimore, MD 21218.
E-mail: zaitchik@jhu.edu

DOI: 10.1175/JHM-D-12-069.1

© 2013 American Meteorological Society

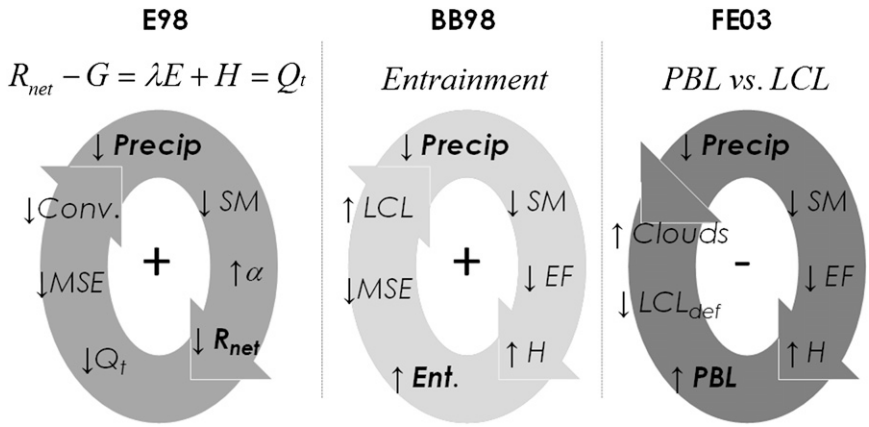

FIG. 1. E98, BB98, and FE03 soil moisture–precipitation feedback pathways; R_{net} = net surface radiation, G = ground heat flux, λE = latent heat flux, H = sensible heat flux, α = surface albedo, Q_t = total land–atmosphere turbulent heat flux, MSE = moist static energy, Conv. = convection, Ent. = entrainment, LCL_{def} = LCL deficit (LCL height − PBL depth), SM = soil moisture, EF = evaporative fraction, PBL = planetary boundary layer depth, LCL = lifting condensation level height.

Climatology Project (ISLSCP) Field Experiment (FIFE) studies of Eltahir (1998) and Betts and Ball (1998), which described two related mechanisms through which local soil moisture anomalies might influence planetary boundary layer (PBL) stability and precipitation. The Eltahir mechanism (E98) focuses on net surface radiation (R_{net}), emphasizing the fact that dry soils can lead to enhanced surface albedo and, because of surface warming, increase upward emission of terrestrial radiation, which leads to a decrease in R_{net} relative to wet conditions when incoming solar radiation is the same. This decrease results in lower total turbulent heat flux (Q_t) to the PBL, producing a low-energy PBL with reduced convective potential (Fig. 1). The Betts and Ball mechanism (BB98) emphasizes surface energy partitioning and the influence that soil moisture conditions have on heat flux between the PBL and the free atmosphere: a dry surface results in lower evaporative fraction [evaporative fraction (EF) = latent heat flux/total turbulent heat flux], enhanced local heating of the PBL due to high sensible heat flux plus, and a deep, dry PBL with significant entrainment of low moist static energy (MSE) at the top of the PBL. This leads to an elevated lifting condensation level (LCL) and reduced likelihood of precipitation. Note that Fig. 1 is a simplified representation of E98 and BB98 that highlights the differing emphases of the two proposed feedback pathways.

For ease of reading, we have described both the E98 and BB98 mechanisms in terms of drought-enhancing feedback pathways (dry soils leading to reduced precipitation), but they can apply to rainfall-enhancing feedbacks (wet soils leading to increased precipitation) as well. Indeed, the original E98 and BB98 papers phrased the hypothesized feedbacks in terms of elevated soil moisture feedbacks. Recent research has indicated that sensitivity to wet versus dry anomalies is asymmetric, with humid regions showing evidence of stronger positive feedbacks under dry anomalies and semiarid regions exhibiting greater sensitivity to wet anomalies (Hohenegger et al. 2009; Koster et al. 2011). Interestingly, the positive feedback mechanism emphasized by BB98—a deep, dry PBL with an elevated LCL—has also been hypothesized to serve as the basis for a negative precipitation feedback in some contexts: if, under dry conditions, the PBL is deepened more than the LCL is raised, there may be enhanced potential for convective precipitation as the likelihood of thermals in the PBL reaching the LCL and triggering cloud formation is increased (Findell and Eltahir 2003) (FE03 in Fig. 1). Negative feedbacks can also arise if a deficit in soil moisture leads to less frequent formation of shallow clouds, allowing for enhanced surface warming and an increased likelihood of deep convection (Hohenegger et al. 2009).

It is important to note that E98 and BB98 are not mutually exclusive mechanisms. Eltahir (1998) explicitly states that both pathways are valid, and his mechanism does consider the EF and entrainment processes emphasized in BB98. Betts and Ball (1998) recognize net surface energy considerations, but they specifically focus on conditions where albedo does not have a significant impact on R_{net}. Nevertheless, the distinction is important from the perspective of mesoscale model development and interpretation. Insomuch as both R_{net}, including albedo effects, and energy partitioning are potentially important to soil moisture–precipitation

feedbacks, modeling studies of land–atmosphere feedbacks must be clear regarding which mechanisms the model is structurally capable of simulating and how this might influence estimated climate sensitivity to land–atmosphere interactions. This matter is particularly important when mesoscale models are applied to project local climate change. In regions where soil-moisture-mediated feedbacks influence seasonality or the development of extremes, the representation of these processes within a modeling system may impact model-based predictions relevant to adaptation.

The sensitivity of mesoscale atmospheric simulations to land surface parameterizations within regional climate models has been a subject of considerable investigation in its own right (Santanello et al. 2009). Such studies are quite valuable to the model development community, but they are unwieldy to perform and difficult for single investigators to replicate. The National Aeronautics and Space Administration (NASA) Unified Weather Research and Forecasting Model (NU-WRF) is designed to facilitate coupled simulations with a range of models and parameter datasets. For the land surface, NU-WRF couples WRF (Skamarock and Klemp 2008) with the Land Information System (LIS; Kumar et al. 2006), allowing for rapid integration of different land surface models, data assimilation schemes, and altered model parameterizations to coupled regional simulations.

Here we present the first seasonal-scale NU-WRF simulation. The system was used to analyze land–atmosphere feedback processes in summer months of the 2005/06 SGP drought (Dong et al. 2011). As the standard WRF system has no land surface physics option that simulates the influence of soil moisture on surface albedo, and therefore structurally excludes the shortwave component of E98 feedbacks related to surface soil moisture, we compare a simulation that uses standard Noah land surface model (Noah LSM) (Chen and Avissar 1994; Ek et al. 2003) physics—that is, no dynamic albedo—with a simulation that includes a simple dynamic albedo routine, implemented to Noah LSM within LIS. Both simulations are compared to a fixed soil moisture simulation that does not allow for any soil-moisture-mediated feedbacks.

2. Methods

NU-WRF v3–3.2.1 was implemented using Goddard long- and shortwave radiation and microphysics routines, the Yonsei University (YSU) PBL scheme (Hong et al. 2006), Noah LSM v3.2 in LIS v6.2 (Kumar et al. 2006), and no cumulus parameterization. Land surface states were spun up offline for 14 years using North American Land Data Assimilation System (NLDAS) forcing (Mitchell et al. 2004) using standard Noah LSM v3.2 physics options. Spinup was identical for all simulations included in this study. Coupled simulations implemented at 4-km resolution were performed for 1 April–1 August 2006. This period coincides with the summer months of the 2005/06 SGP drought. Extensive soil moisture anomalies were observed, with associated albedo anomalies in the areas of most severe drought. A second set of simulations was performed for 1 April–1 August 2007 to provide a contrast between the drought year and a wet year (Fig. 2). Lateral boundary conditions for all simulations were drawn from the 12-km-resolution North American Mesoscale Model (NAM; http://nomads.ncdc.noaa.gov/data.php).

Three simulations were performed: a soil moisture memory (SMM) experiment, in which soil moisture states were allowed to evolve throughout the course of the simulation; a no soil memory (NSM) experiment, in which soil moisture was fixed at initial values; and a soil memory with albedo (SMA) simulation, in which Noah was enhanced with a simple albedo routine that predicts surface snow-free albedo (α) in nonurban areas as a function of near-surface soil moisture ($\theta_{10\mathrm{cm}}$) and green vegetation fraction (f_c):

$$\alpha = \alpha_{\mathrm{LUT}} - 0.0025(1 - f_c)(\theta_{10\mathrm{cm}} - \overline{\theta_{10\mathrm{cm}}}),$$

where α_{LUT} is Noah LSM default snow-free albedo (a function of land cover) and $\overline{\theta_{10\mathrm{cm}}}$ is climatological summertime soil moisture. The relationship was derived using optimal linear correlations between Moderate Resolution Imaging Spectroradiometer (MODIS) broadband shortwave (0.3–5.0 μm) white sky albedo estimates (MCD43C3; Schaaf et al. 2002) and offline Noah-simulated soil moisture for April–July over 12 years (2000–11), adjusted for f_c. This albedo routine is intended as a proof of concept that will require further refinement. Conceptually, it is similar to empirical albedo estimation schemes derived in previous observational and modeling studies (Guan et al. 2009; Matsui et al. 2007; Roxy et al. 2010). The NSM and SMM simulations used monthly Advanced Very High Resolution Radiometer (AVHRR) snow-free albedo climatology, which has a native resolution of 0.25° (data are available online at http://daac.ornl.gov/cgi-bin/dsviewer.pl?ds_id=959). All simulations used climatological monthly values for f_c. The influence of time-evolving f_c anomalies on NU-WRF simulations and the sensitivity of coupling behavior to model physics are subjects of complementary studies (Santanello et al. 2013).

3. Simulation results

NU-WRF provided stable and realistic simulations of the SGP over the course of the 4-month simulation

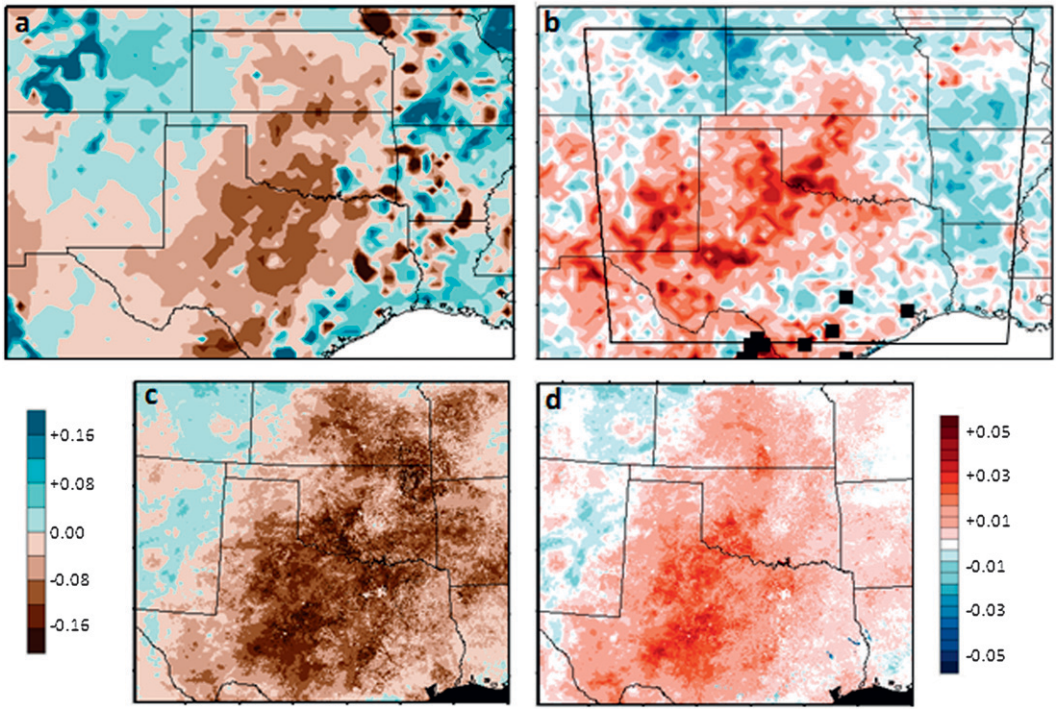

FIG. 2. Difference in (a) Advanced Microwave Scanning Radiometer for Earth Observing System (AMSR-E) Land Parameter Retrieval Model (LPRM) soil moisture (Owe et al. 2008), (b) MODIS MCD43C3 white sky albedo anomaly (Schaaf et al. 2002), (c) NU-WRF top 10-cm soil moisture from the SMA simulation, and (d) NU-WRF SMA surface albedo between July 2006 and July 2007. Box in (b) indicates the NU-WRF modeling domain in this study.

period, including the spatial distribution of soil moisture and albedo anomalies when these fields were simulated (Figs. 2c,d). The NU-WRF simulation without soil moisture memory (NSM) overestimated precipitation throughout the drought-affected region of the SGP (Fig. 3)—where ''drought affected'' is defined as all areas and times in which simulated near-surface (top 10 cm) soil moisture deficit was larger in the interactive soil moisture simulation (i.e., SMM or SMA) than in the fixed soil moisture experiment (NSM)—while simulations with soil moisture memory yielded a closer match to observations. Notably, the simulations differed primarily in the yield and location of each precipitation event rather than in the frequency of rain occurrence; the number of wet days in the drought-affected region as a whole was nearly identical in all three simulations. Adding active albedo (SMA) to NU-WRF had no statistically significant impact on total precipitation in the drought-affected region, but it did cause additional redistribution of precipitation from regions of soil moisture deficit—and therefore generally elevated albedo in SMA—to regions of higher soil moisture and reduced albedo, as discussed below. There was also a systematic difference in the diurnal cycle of precipitation between SMA and SMM. The reduction in precipitation in SMM relative to NSM in drought-affected areas is primarily a product of reduced nighttime precipitation, while the percentwise reduction in precipitation in SMA relative to NSM is greatest during daytime hours (Fig. 4). Comparing SMA to SMM, the SMA (SMM) simulation produced more nighttime (daytime) precipitation. Comparisons with air temperature at select meteorological stations within the drought-affected area showed no significant bias in daily temperature over the full course of the simulations, though NSM did develop a small cold bias in later months that was not observed in SMM or SMA.

The influence of SMM and SMA on states and fluxes relevant to soil moisture feedbacks are summarized in Table 1. In this table, low soil moisture zones (LM) are defined as areas in which $\theta_{0\text{–}10\text{cm}}$ (SMM) $<$ $\theta_{0\text{–}10\text{cm}}$ (NSM), while high soil moisture zones (HM) are areas with $\theta_{10\text{cm}}$ (SMM) $>$ $\theta_{10\text{cm}}$ (NSM). Similarly, high albedo zones (HA) are areas with $\alpha_{\text{SMA}} > \alpha_{\text{SMM}}$, and low albedo zones (LA) have $\alpha_{\text{SMA}} < \alpha_{\text{SMM}}$. Note that HA and LM zones are not entirely overlapping on account of differences in the evolution of near-surface soil moisture between SMA and SMM simulations. SMM exhibited

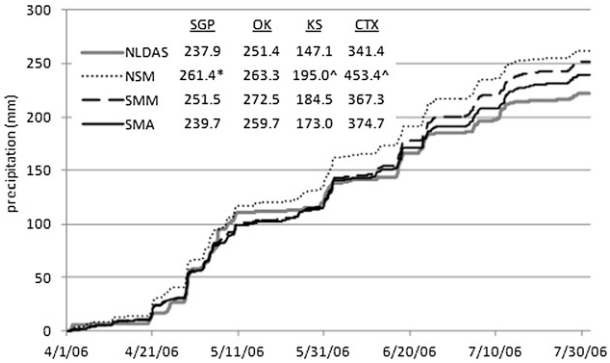

FIG. 3. Cumulative precipitation in NU-WRF simulations and the NLDAS observation-based analysis for the drought-affected region of the SGP. Also shown are the April–July precipitation totals (mm) for the drought-affected portion of the SGP, Oklahoma (OK), Kansas (KS), and central Texas (CTX). Significant differences between simulation and NLDAS in decad precipitation–paired t test, accounting for temporal autocorrelation, are indicated for $p < 0.05$ (*) and $p < 0.1$ (^).

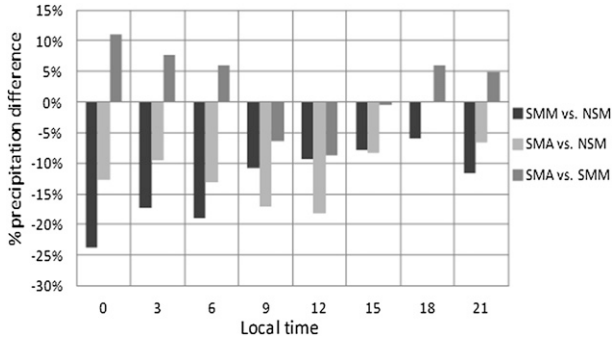

FIG. 4. Diurnal pattern in % precipitation difference between NU-WRF simulations, summed for the entire April–July 2006 simulation period over drought-affected areas of the SGP.

a deeper daytime PBL and LCL, substantially lower maximum vertically integrated CAPE (MCAPE; calculated as the maximum integrated CAPE for any starting height in the PBL), and lower day and night MSE than NSM in low soil moisture zones (LM), where MSE is calculated as the local PBL average. The contrast in moist static energy reaches a maximum at night owing to integrated effects of daytime fluxes on the residual PBL. Moisture was reduced regionwide in SMM relative to NSM, so some reduction in MSE is observed in high soil moisture zones (HM) as well as LM zones, but the simulations do not show any tendency toward reduced nighttime precipitation in the HM areas.

The introduction of dynamic albedo to NU-WRF (SMA compared to SMM) led to stronger precipitation contrasts between areas where drought-induced surface brightening (HA) and relatively wetter areas where the simulated surface albedo was reduced relative to baseline (LA). Over the course of the entire simulation (April–July) for the entire SGP analysis region, SMA produced significantly more precipitation than SMM in LA zones (total area averaged difference = 43.3 mm) and significantly less in HA zones (−37.2 mm). These differences were primarily a product of differences in the yield of each precipitation event. The SMA and SMM simulations show very nearly the same timing of precipitation events and approximately the same relative magnitude of events (r^2 for regionwide 3-hourly precipitation rate in SMA and SMM was 0.88 in HA and 0.96 in LA zones)—patterns that indicate that differences between SMA and SMM are secondary modifications of larger-scale precipitation processes. The absolute yield of precipitation events differed systematically, with SMA yielding 6.6% more precipitation per event in the LA zone and 22% less precipitation per event in the HA zone. These precipitation differences were associated with enhanced net surface radiation (R_{net}) and total turbulent energy transfer (Q_t) in LA areas and reduced values in HA areas in the SMA simulation. These simulated surface energy effects appeared across the SGP, but they were most dramatic in the core drought region. For this reason, we focus our discussion of albedo feedbacks, including the figures presented in Table 1, on midsummer (June–July) effects in Oklahoma.

4. Simulated feedback mechanisms

NSM overestimated precipitation relative to NLDAS observation-based analysis, while SMM produced less precipitation in drought-affected areas and slightly improved comparison with observations. The redistribution of precipitation from low- to high-moisture areas is consistent with a positive precipitation feedback—a result that is consistent with theoretical studies and with some modeling investigations (Findell and Eltahir 2003; Koster et al. 2004; Schär et al. 1999; Seneviratne et al. 2010; Zaitchik et al. 2007), though it differs from the negative feedbacks found in some other studies, including the cloud-resolving simulations by Hohenegger et al. (2009). These differences are likely due to a combination of contrasting regional atmospheric conditions—Hohenegger et al. (2009) studied a humid, mountainous area in Europe—but they may also be a product of different modeling systems and sensitivity experiments.

The mechanism through which SMM-simulated reduced precipitation is consistent with BB98 (see Fig. 1). In LM areas, the SMM simulation had low evaporative fraction (EF) and high sensible heat flux (Q_h) relative to NSM, leading to a deep PBL. This PBL is low energy because it is deep and has entrained low-energy air from

TABLE 1. Difference in daily average, midday (1800 UTC), and night (0600 UTC) values for selected variables, as simulated by NU-WRF. Differences between NSM and SMM are shown for HM vs LM areas for the entire April–July 2006 simulation period, averaged over the SGP, while SMM and SMA are compared for HA vs LA areas in June–July, the period of maximum albedo-mediated feedback, in Oklahoma. Parameter definitions are θ = root zone volumetric soil moisture, SW_{in} = surface incoming shortwave radiation, T_{surf} = surface temperature, R_{net} = net surface radiation, Q_{le} = latent heat flux, Q_h = sensible heat flux, EF = evaporative fraction, Q_t = turbulent heat flux ($Q_{le} + Q_h$), PBLH = height of the PBL, LCLH = height of LCL, MCAPE = CAPE for parcel with maximum equivalent potential energy in the column, LCL deficit = LCLH − PBLH (Santanello et al. 2009), ⟨MSE⟩ = moist static energy density. Bold type indicates significance at $p < 0.05$ for paired t test on daily values, accounting for temporal autocorrelation.

		SMM-NSM HM	SMM-NSM LM	SMA-SMM LA	SMA-SMM HA
24 h	Total rain (mm)	**74.2**	**−29.8**	**62.8**	**−37.2**
	θ ($m^3\ m^{-3}$)	**0.03**	**−0.06**	0.00	**−0.01**
	Albedo	0.000	0.000	**−0.033**	**0.015**
Midday	SW_{in} ($W\ m^{-2}$)	−3.1	0.1	−4.0	3.6
	T_{surf} (K)	**−1.5**	**1.8**	**0.5**	**0.1**
	R_{net} ($W\ m^{-2}$)	**4.8**	**−10.0**	**20.3**	**−12.2**
	Q_{le} ($W\ m^{-2}$)	**25.1**	**−41.3**	2.0	**−13.8**
	Q_h ($W\ m^{-2}$)	**−28.3**	**28.9**	**13.1**	**3.4**
	EF	**0.07**	**−0.09**	−0.01	**−0.02**
	Q_t ($W\ m^{-2}$)	−3.2	**−12.4**	**15.1**	**−10.4**
	PBLH (m)	**−76.5**	**109.2**	9.5	−0.6
	LCLH (m)	**−89.4**	**147.7**	2.6	9.3
	MCAPE ($J\ kg^{-1}$)	9.1	**−95.0**	9.0	−3.2
	LCL deficit (m)	−12.9	**38.5**	−7.0	10.0
	⟨MSE⟩ ($kJ\ kg^{-1}$)	−0.1	**−0.8**	0.0	**−0.1**
Night	PBLH (m)	**−62.8**	−7.1	8.9	**7.0**
	LCLH (m)	−38.3	78.9	10.6	5.1
	MCAPE ($J\ kg^{-1}$)	**−19.1**	**−40.8**	−6.8	−4.1
	LCL deficit (m)	24.4	**86.0**	1.8	−2.1
	⟨MSE⟩ ($kJ\ kg^{-1}$)	**−0.8**	**−1.1**	0.1	0.0

the free troposphere—a mechanism emphasized in BB98—and because high surface temperatures led to elevated emission of terrestrial radiation and, therefore, reduced R_{net} and lower total turbulent heat flux (Q_t) into the PBL. This Q_t-mediated process is consistent with the longwave component of the E98 pathway—reduced R_{net} leads to a low-energy PBL—and reinforces the positive drought feedback. The land–atmosphere coupling processes responsible for a low-energy, stable PBL are most active during the daytime, but the tendency persists in the residual nocturnal boundary layer, particularly as relatively warm surface conditions and low PBL humidity in SMM relative to NSM facilitate nighttime dissipation of energy through emission of terrestrial radiation. As a result, precipitation was reduced in SMM at all hours. While the simulated deepening of the daytime PBL in SMM relative to NSM under low soil moisture conditions has the potential to produce a negative precipitation feedback—that is, increased precipitation due to increased probability of the PBL deepening to the LCL (Findell and Eltahir 2003; Hohenegger et al. 2009)—this potential was not realized in WRF simulations. In LM areas, SMM led to a dramatically elevated LCL height relative to NSM, such that the LCL deficit was greater in SMM than NSM during both day and night. In the HM zone the LCL deficit was reduced in SMM relative to NSM, as expected, during the day. At night there was a nonsignificant tendency toward increased LCL deficit but there was no evidence of a negative precipitation feedback, as precipitation in SMM exceeded precipitation in NSM during nighttime hours in HM areas.

In comparison to the energy partitioning soil moisture precipitation feedback described above, contrasts due to the introduction of active albedo (SMA versus SMM) are of a different and more subtle character. As shown in Table 1, there is a significant redistribution of precipitation from HA to LA areas when active albedo (SMA) is included in WRF simulations in the Oklahoma focus area. This redistribution is associated with net energy effects that are consistent with the E98 feedback pathway: in HA areas, SMA leads to reduced net surface energy (R_{net}) and total turbulent energy transfer (Q_t) relative to SMM, and the opposite is true in LA areas. The magnitude of these differences—on the order of 10–15 $W\ m^{-2}$ for average midday conditions in Oklahoma—is approximately the same as observed differences due to soil moisture reported in E98. This difference is primarily a direct product of the relationship between soil moisture and albedo, which is

a process that is structurally excluded from standard versions of WRF.

While these differences in surface fluxes due to albedo are apparent in the temporal and spatial average, the critical coupling links proposed by E98 and others are not: average differences in MSE density, CAPE, and LCL deficit are insignificant in the Oklahoma focus region (Table 1) and in the SGP on the whole. The coupling mechanism is only evident when one focuses on times and locations amenable to precipitation events. The average difference in boundary layer MSE density between SMA and SMM for locations that are within 24 h of the onset of a simulated precipitation event is $+0.4$ kJ kg^{-1} in LA zones and -0.1 kJ kg^{-1} in HA zones (both differences significant at $\alpha = 0.05$), and the average differences in CAPE are $+44.5$ J kg^{-1} in LA—with local transient differences as large as 1358 J kg^{-1}—and -14.0 J kg^{-1} in HA, with transient differences as large as -569 J kg^{-1} (LA is statistically significant at $\alpha = 0.05$). The magnitude of these calculated differences is moderated by the fact that our analysis considers a long period of drought over a large area, and thus includes a considerable amount of synoptic and mesoscale diversity. Nevertheless, the differences are systematic and statistically significant, and they are consistent with an E98 type feedback pathway in which albedo anomalies influence net radiation and total heat flux, leading to an increase in PBL energy when albedo is reduced and a decrease when albedo is elevated. As in E98, we find an association between these energetic influences of albedo and local precipitation. Differences in PBL depth are uniform across HA and LA even for these prerain periods, indicating that total heat flux, and not PBL depth effects, are the primary pathway through which active albedo modifies the yield of precipitation events in these simulations.

5. Conclusions

Regional climate models are a critical tool for forecasts and downscaling future climate projections. Future climate applications have received particular attention recently, as researchers attempt to project the impacts of anthropogenic climate change at scales relevant to decision makers. One reason that regional climate models are employed in this task is that they are capable of capturing nonstationary climate change processes, in which the relationship between large-scale circulations and local conditions changes as a function of evolving background conditions. Soil moisture feedbacks are salient examples of local processes subject to nonstationary behavior under climate change. As climate zones migrate under changes in global temperature and precipitation patterns, the nature of land–atmosphere coupling and feedbacks will likely change as well. Insomuch as these feedbacks impact local climate—as they are believed to in many regions—it is important to represent all feedback pathways as realistically as possible. This need has been recognized by some independent regional climate modeling efforts, such as Climate WRF (CWRF; Liang et al. 2012), but it has not been a focus for mainstream WRF development.

Here, we have used NU-WRF to examine the impact of a simple soil-moisture-mediated dynamic albedo scheme on WRF simulations of drought at seasonal scale. It was found that for the 2006 SGP drought, dynamic albedo influenced the spatial pattern and diurnal distribution of simulated precipitation in a manner that is consistent with hypothesized feedback pathways. The albedo routine did not, however, have a significant impact on regionally averaged precipitation and thus was not critical to large-scale drought analysis in this application; impacts were only significant when considering the simulation of subregional precipitation patterns. In focusing solely on the soil-moisture-mediated aspects of surface albedo and energy partitioning, we have neglected the role that changes in vegetation cover are expected to play in drought feedbacks. Integrating satellite-derived green vegetation fraction into NU-WRF is the subject of a complementary study, and these results will inform the implementation of combined dynamic albedo and time-evolving vegetation routines within NU-WRF, utilizing the system's potential as a test bed for modeling land–atmosphere interactions affecting weather and climate.

Acknowledgments. This work was supported by NASA Modeling, Analysis, and Prediction Program Grant NNX09AU61G. We also thank three anonymous reviewers for their helpful comments on the original manuscript.

REFERENCES

Betts, A. K., 2009: Land-surface-atmosphere coupling in observations and models. *J. Adv. Model. Earth Syst.,* **1** (1), 1–18.

——, and J. H. Ball, 1998: FIFE surface climate and site-average dataset 1987–89. *J. Atmos. Sci.,* **55,** 1091–1108.

Charney, J., W. J. Quirk, S. H. Chow, and J. Kornfield, 1977: Comparative study of effects of albedo change on drought in semi-arid regions. *J. Atmos. Sci.,* **34,** 1366–1385.

Chen, F., and R. Avissar, 1994: Impact of land-surface moisture variability on local shallow convective cumulus and precipitation in large-scale models. *J. Appl. Meteor.,* **33,** 1382–1401.

Dirmeyer, P. A., R. D. Koster, and Z. Guo, 2006: Do global models properly represent the feedback between land and atmosphere? *J. Hydrometeor.,* **7,** 1177–1198.

Dong, X., and Coauthors, 2011: Investigation of the 2006 drought and 2007 flood extremes at the Southern Great Plains through an integrative analysis of observations. *J. Geophys. Res.,* **116,** D03204, doi:10.1029/2010JD014776.

Ek, M. B., K. E. Mitchell, Y. Lin, E. Rogers, P. Grunmann, V. Koren, G. Gayno, and J. D. Tarpley, 2003: Implementation of Noah land surface model advances in the National Centers for Environmental Prediction operational mesoscale Eta model. *J. Geophys. Res.,* **108,** 8851, doi:10.1029/2002JD003296.

Eltahir, E. A. B., 1998: A soil moisture rainfall feedback mechanism: 1. Theory and observations. *Water Resour. Res.,* **34,** 765–776.

Findell, K. L., and E. A. B. Eltahir, 2003: Atmospheric controls on soil moisture–boundary layer interactions. Part II: Feedbacks within the continental United States. *J. Hydrometeor.,* **4,** 570–583.

Guan, X., J. Huang, N. Guo, J. Bi, and G. Wang, 2009: Variability of soil moisture and its relationship with surface albedo and soil thermal parameters over the Loess Plateau. *Adv. Atmos. Sci.,* **26,** 692–700.

Hohenegger, C., P. Brockhaus, C. S. Bretherton, and C. Schar, 2009: The soil moisture–precipitation feedback in simulations with explicit and parameterized convection. *J. Climate,* **22,** 5003–5020.

Hong, S.-Y., Y. Noh, and J. Dudhia, 2006: A new vertical diffusion package with an explicit treatment of entrainment processes. *Mon. Wea. Rev.,* **134,** 2318–2341.

Koster, R. D., and Coauthors, 2004: Regions of strong coupling between soil moisture and precipitation. *Science,* **305,** 1138–1140.

——, and Coauthors, 2011: The second phase of the Global Land–Atmosphere Coupling Experiment: Soil moisture contributions to subseasonal forecast skill. *J. Hydrometeor.,* **12,** 805–822.

Kumar, S. V., and Coauthors, 2006: Land information system: An interoperable framework for high resolution land surface modeling. *Environ. Modell. Software,* **21,** 1402–1415.

Liang, X.-Z., and Coauthors, 2012: Regional climate–Weather Research and Forecasting model. *Bull. Amer. Meteor. Soc.,* **93,** 1363–1387.

Matsui, T., A. Beltrán-Przekurat, R. A. Pielke Sr., D. Niyogi, and M. B. Coughenour, 2007: Continental-scale multiobservation calibration and assessment of Colorado State University Unified Land Model by application of Moderate Resolution Imaging Spectroradiometer (MODIS) surface albedo. *J. Geophys. Res.,* **112,** G02028, doi:10.1029/2006JG000229.

Meng, X. H., J. P. Evans, and M. F. McCabe, 2011: Numerical modelling and land–atmosphere feedback of drought in southeast Australia. IAHS Publ. 344, 144–149.

Mitchell, K. E., and Coauthors, 2004: The multi-institution North American Land Data Assimilation System (NLDAS): Utilizing multiple GCIP products and partners in a continental distributed hydrological modeling system. *J. Geophys. Res.,* **109,** D07S90, doi:10.1029/2003JD003823.

Notaro, M., Z. Liu, and J. W. Williams, 2006: Observed vegetation–climate feedbacks in the United States. *J. Climate,* **19,** 763–786.

Owe, M., R. de Jeu, and T. Holmes, 2008: Multisensor historical climatology of satellite-derived global land surface moisture. *J. Geophys. Res.,* **113,** F01002, doi:10.1029/2007JF000769.

Pielke, R. A., R. L. Walko, L. T. Steyaert, P. L. Vidale, G. E. Liston, W. A. Lyons, and T. N. Chase, 1999: The influence of anthropogenic landscape changes on weather in south Florida. *Mon. Wea. Rev.,* **127,** 1663–1673.

Roxy, M., V. Sumithranand, and G. Renuka, 2010: Variability of soil moisture and its relationship with surface albedo and soil thermal diffusivity at Astronomical Observatory, Thiruvananthapuram, south Kerala. *J. Earth Syst. Sci.,* **119,** 507–517.

Santanello, J. A., C. D. Peters-Lidard, S. V. Kumar, C. Alonge, and W.-K. Tao, 2009: A modeling and observational framework for diagnosing local land–atmosphere coupling on diurnal time scales. *J. Hydrometeor.,* **10,** 577–599.

——, ——, and ——, 2011: Diagnosing the sensitivity of local land–atmosphere coupling via the soil moisture–boundary layer interaction. *J. Hydrometeor.,* **12,** 766–786.

——, ——, A. Kennedy, and S. V. Kumar, 2013: Diagnosing the nature of land–atmosphere coupling: A case study of the dry/wet extremes in the U.S. southern Great Plains. *J. Hydrometeor.,* **14,** 3–24.

Schaaf, C. B., and Coauthors, 2002: First operational BRDF, albedo nadir reflectance products from MODIS. *Remote Sens. Environ.,* **83,** 135–148.

Schär, C., D. Lüthi, U. Beyerle, and E. Heise, 1999: The soil–precipitation feedback: A process study with a regional climate model. *J. Climate,* **12,** 722–741.

Seneviratne, S. I., and R. Stockli, 2008: The role of land–atmosphere interactions for climate variability in Europe. *Climate Variability and Extremes during the Past 100 Years,* S. Bronnimann et al., Eds., Springer, 179–193.

——, and Coauthors, 2006: Soil moisture memory in AGCM simulations: Analysis of Global Land–Atmosphere Coupling Experiment (GLACE) data. *J. Hydrometeor.,* **7,** 1090–1112.

——, T. Corti, E. L. Davin, M. Hirschi, E. B. Jaeger, I. Lehner, B. Orlowsky, and A. J. Teuling, 2010: Investigating soil moisture–climate interactions in a changing climate: A review. *Earth-Sci. Rev.,* **99,** 125–161.

Skamarock, W. C., and J. B. Klemp, 2008: A time-split nonhydrostatic atmospheric model for weather research and forecasting applications. *J. Comput. Phys.,* **227,** 3465–3485.

Taylor, C. M., and T. Lebel, 1998: Observational evidence of persistent convective-scale rainfall patterns. *Mon. Wea. Rev.,* **126,** 1597–1607.

Teuling, A. J., and Coauthors, 2009: A regional perspective on trends in continental evaporation. *Geophys. Res. Lett.,* **36,** L02404, doi:10.1029/2008GL036584.

——, and Coauthors, 2010: Contrasting response of European forest and grassland energy exchange to heatwaves. *Nat. Geosci.,* **3,** 722–727.

Weaver, C. P., S. B. Roy, and R. Avissar, 2002: Sensitivity of simulated mesoscale atmospheric circulations resulting from landscape heterogeneity to aspects of model configuration. *J. Geophys. Res.,* **107,** 8041, doi:10.1029/2001JD000376.

Zaitchik, B. F., J. P. Evans, R. A. Geerken, and R. B. Smith, 2007: Climate and vegetation in the Middle East: Interannual variability and drought feedbacks. *J. Climate,* **20,** 3924–3941.